



Short communication

A flat-tubular solid oxide fuel cell with a dense interconnect film coated on the porous anode support

Beom-Kyeong Park^{a,b}, Jong-Won Lee^{a,b,*}, Seung-Bok Lee^a, Tak-Hyoung Lim^a, Seok-Joo Park^a, Rak-Hyun Song^a, Dong-Ryul Shin^a

^a Fuel Cell Research Center, Korea Institute of Energy Research, 152 Gajeong-ro, Yuseong-gu, Daejeon 305-343, Republic of Korea

^b Department of Advanced Energy Technology, University of Science and Technology, 217 Gajeong-ro, Yuseong-gu, Daejeon 305-350, Republic of Korea

ARTICLE INFO

Article history:

Received 9 March 2012

Received in revised form

10 April 2012

Accepted 13 April 2012

Available online 21 April 2012

Keywords:

Solid oxide fuel cell

Flat-tubular cell

Anode support

Ceramic interconnect

Sintering

ABSTRACT

An interconnect in an anode-supported flat-tubular solid oxide fuel cell (SOFC) electrically connects unit cells and separates fuel and oxidant gases in a stack. An anode-supported flat-tubular SOFC with a highly conductive and dense interconnect film is developed. The dense interconnect film having an n-type conducting layer on the reducing side and a p-type conducting layer on the oxidizing side is fabricated on a porous anode support by a simple and cost-effective screen-printing process, followed by co-sintering with the anode and the electrolyte. The interconnect exhibits low resistance and high stability in a dual atmosphere. The anode-supported flat-tubular cell with the ceramic interconnect shows a power density as high as 360 mW cm^{-2} at 850°C .

© 2012 Elsevier B.V. All rights reserved.

1. Introduction

An anode-supported flat-tubular solid oxide fuel cell (SOFC) design is an advanced cell configuration, which offers many advantages including a high volumetric power density, a minimized sealing area and a high resistance to thermal cycling [1–4]. Multiple cells are connected in electrical series to increase the output voltage of the SOFC system. In a stack, an interconnect electrically connects unit cells and separates fuel from oxidant in the adjoining cells. As shown in Fig. 1, the flat-tubular design requires a thin interconnect film coated on a porous anode support. This interconnect film should be not only impermeable to gases, but also conductive and stable in a dual atmosphere (reducing atmosphere on the anode side and oxidizing atmosphere on the cathode side).

Ca or Sr-doped LaCrO_3 materials are commonly used for SOFC interconnects, because they show acceptable conductivity and stability in the fuel cell environment [5,6]. There are, however, two major issues that need to be addressed: (i) the doped LaCrO_3 is

a p-type conductor whose conductivity drops significantly under reducing conditions on the anode side [6]. This results in an increased interconnect resistance in the dual atmosphere. (ii) It is quite difficult to fabricate a dense interconnect film on a porous anode support by using conventional powder-sintering processes. The poor sinterability of doped LaCrO_3 is due to the vaporization of gaseous Cr–O species and the migration of transient liquid phases (e.g. CaCrO_4 and SrCrO_4) into the porous substrate during sintering [7,8]. For this reason, LaCrO_3 interconnect films have typically been fabricated using relatively expensive and complicated deposition techniques, e.g. electrochemical vapor deposition [9] and plasma spraying [10,11].

This paper reports a way to fabricate an anode-supported flat-tubular SOFC with a highly conductive and dense interconnect film. The key features of the approach used to address the problems mentioned above may be summarized as follows: (i) the interconnect film consists of an n-type conducting $\text{Sr}_{0.7}\text{La}_{0.2}\text{TiO}_3$ layer on the anode side (exposed to a reducing atmosphere) and a p-type conducting $\text{La}_{0.8}\text{Sr}_{0.2}\text{MnO}_3$ layer on the cathode side (exposed to an oxidizing atmosphere). Huang and Gopalan [12] have theoretically demonstrated that the interconnect can be designed with high conductivity in both reducing and oxidizing atmospheres by selection of appropriate n- and p-type materials and control of the thickness of each layer. A previous study [4] showed that Sr-

* Corresponding author. Fuel Cell Research Center, Korea Institute of Energy Research, 152 Gajeong-ro, Yuseong-gu, Daejeon 305-343, Republic of Korea. Tel.: +82 42 860 3025; fax: +82 42 860 3297.

E-mail address: jjong277@kier.re.kr (J.-W. Lee).

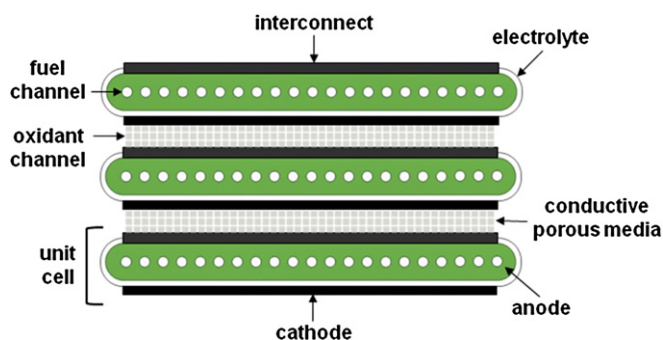


Fig. 1. Schematic diagram of anode-supported flat-tubular SOFCs connected in electrical series. A thin interconnect film is coated on one side of unit cell.

deficient $\text{Sr}_{0.7}\text{La}_{0.2}\text{TiO}_3$ is a promising interconnect material with an n-type conducting property due to its high conductivity, good sinterability and thermal compatibility with Ni-YSZ anodes. (ii) The Pechini-derived, nano-sized powders of $\text{Sr}_{0.7}\text{La}_{0.2}\text{TiO}_3$ and $\text{La}_{0.8}\text{Sr}_{0.2}\text{MnO}_3$ with improved sinterability are used to fabricate the dense interconnect film on the porous anode. (iii) The interconnect film is fabricated by a simple screen-printing process, followed by co-sintering with the anode and the electrolyte. This provides benefits in reducing the number of fabrication steps and in cost saving.

2. Experimental

2.1. Preparation of interconnect materials and screen-printing pastes

Nano-sized $\text{Sr}_{0.7}\text{La}_{0.2}\text{TiO}_3$ and $\text{La}_{0.8}\text{Sr}_{0.2}\text{MnO}_3$ powders were prepared by the Pechini method using citric acid. Briefly, the metal precursors, $\text{Sr}(\text{NO}_3)_2$, $\text{La}(\text{NO}_3)_3 \cdot 6\text{H}_2\text{O}$, $\text{Ti}(\text{OCH}(\text{CH}_3)_2)_4$, and $\text{Mn}(\text{CH}_3\text{COO})_2 \cdot 4\text{H}_2\text{O}$, were dissolved in ethylene glycol. Citric acid was added to the solution under stirring conditions, and the mixture was heated to 150°C to form a viscous gel. The gel was dried at 250°C and then calcined in a temperature range from 800 to 1000°C for 5 h to remove any remaining organic materials. Spherical particles as large as 50 – 80 nm were produced for both $\text{Sr}_{0.7}\text{La}_{0.2}\text{TiO}_3$ and $\text{La}_{0.8}\text{Sr}_{0.2}\text{MnO}_3$. The screen-printing paste was prepared by mixing the powder with ethyl cellulose and α -terpinol.

2.2. Cell fabrication

An anode support was fabricated by extrusion of the powder mixture: NiO, 8 mol.% Y_2O_3 -stabilized ZrO_2 (YSZ), activated carbon (YP-50F) and organic binder (YB-131D). The extruded support was pre-sintered at 1100°C . An anode functional layer (AFL) of NiO-YSZ ($15\ \mu\text{m}$ in thickness) was coated onto the pre-sintered support by a dip-coating process, and then sintered at 1000°C . One side of the anode support was partially masked for interconnect coating, and then a YSZ electrolyte layer (thickness $\sim 8\ \mu\text{m}$) was formed by the vacuum slurry coating process [13]. For interconnect fabrication, the $\text{Sr}_{0.7}\text{La}_{0.2}\text{TiO}_3$ paste was screen-printed onto the surface of the anode support without the coated electrolyte layer, followed by the coating of $\text{La}_{0.8}\text{Sr}_{0.2}\text{MnO}_3$. The interconnect-coated half-cell was co-sintered at 1400°C . Finally, a multi-layered cathode (thickness $\sim 25\ \mu\text{m}$) composed of (i) $(\text{La}_{0.85}\text{Sr}_{0.15})_{0.9}\text{MnO}_3$ -YSZ composite, (ii) $(\text{La}_{0.85}\text{Sr}_{0.15})_{0.9}\text{MnO}_3$ and (iii) $\text{La}_{0.6}\text{Sr}_{0.4}\text{Co}_{0.2}\text{Fe}_{0.8}\text{O}_3$ was coated onto the co-sintered tube by a dip-coating process and, then, it was sintered at 1150°C .

2.3. Characterization of interconnect layer and unit cell

The coated interconnect film was characterized by scanning electron microscopy (SEM, Hitach X-4900) coupled with energy dispersive spectroscopy (EDS). The area-specific resistance (ASR) of the interconnect film coated on the anode support was measured by a DC four-probe technique (Keithley 2400). H_2 and air were supplied to the $\text{Sr}_{0.7}\text{La}_{0.2}\text{TiO}_3$ and $\text{La}_{0.8}\text{Sr}_{0.2}\text{MnO}_3$ sides of the interconnect film, respectively. The sample was heated to 900°C and then held until a steady-state condition was attained. After that, the conductivity was evaluated over a temperature range of 700 – 900°C . A unit cell was mounted with metal tubes for H_2 supply using a ceramic adhesive. For current collection, Pt meshes were attached onto the surfaces of the interconnect and cathode using a Pt paste and, then, Pt wires were connected to the Pt meshes. See Fig. S1 for the fuel cell testing set-up in the Supplementary Data. The polarization curves of the unit cell were measured with a fully automated fuel cell station using H_2 gas with 3 vol.% H_2O at the anode and air at the cathode.

3. Results and discussion

Fig. 2a presents the anode-supported flat-tubular SOFC fabricated in this study. The unit cell was made as a flat tube ($3.6\ \text{mm}$ thick, $36.2\ \text{mm}$ wide and $150\ \text{mm}$ long) having 20 holes with a diameter of $1\ \text{mm}$ in the anode support. The coated interconnect area is $27.5\ \text{cm}^2$. When the interconnect film was fabricated, the paste composition and the screen-printing conditions were carefully tailored to obtain a dense layer of the desired thickness. Fig. 2b and c show the SEM images of the surface and cross-section of the interconnect film co-sintered with the anode support and the electrolyte at 1400°C , respectively. The dense interconnect film of about $30\ \mu\text{m}$ in thickness was obtained after co-sintering (see Fig. S2 for the SEM images with high magnifications). The thicknesses of the $\text{Sr}_{0.7}\text{La}_{0.2}\text{TiO}_3$ and $\text{La}_{0.8}\text{Sr}_{0.2}\text{MnO}_3$ layers are approximately 10 and $20\ \mu\text{m}$, respectively. Note that each layer contains no connected pores on the surface and across the thickness. The interfaces between the layers were found to be cohesive without cracking or delamination. The EDS analysis in Fig. 2(d) confirms that $\text{Sr}_{0.7}\text{La}_{0.2}\text{TiO}_3$ and $\text{La}_{0.8}\text{Sr}_{0.2}\text{MnO}_3$ did not react with each other to form secondary phases at the interface during the co-sintering process. The results clearly demonstrate that the dense interconnect film can be fabricated on the porous anode by screen-printing and co-sintering of nano-sized powders without any sintering aids. For comparison, an $\text{La}_{0.8}\text{Ca}_{0.2}\text{CrO}_3$ interconnect film was prepared by the same screen-printing and co-sintering process. A very porous skeleton was obtained after sintering at 1400°C (Fig. S3). Improvements in densification of the interconnect film compared with doped LaCrO_3 may be due to the fact that neither gaseous species nor liquid transient phase with low-melting point is formed from the $\text{Sr}_{0.7}\text{La}_{0.2}\text{TiO}_3$ and $\text{La}_{0.8}\text{Sr}_{0.2}\text{MnO}_3$ powders during sintering. Furthermore, the Pechini-derived, fine powders consisting of nano-scale primary particles improves sinterability due to lower temperatures required for densification (Fig. S4).

The SOFC interconnect should possess low electrical resistance to minimize ohmic losses between the electrodes of adjacent cells. The generally accepted limit of ASR is $0.1\ \Omega\ \text{cm}^2$ [5]. Fig. 3a illustrates the ASR values of the interconnect film coated on the porous anode. The ASR values were measured to be 25 to $76\ \text{m}\Omega\ \text{cm}^2$ at temperatures between 700 and 900°C , indicating that the interconnect film had sufficiently low resistance for use as SOFC interconnects. The measured ASR values are comparable to those of some metallic interconnects coated with protective ceramic layers [14]. For comparison, the interconnect film was fabricated with a single $\text{Sr}_{0.7}\text{La}_{0.2}\text{TiO}_3$ layer, and the ASR was measured to be ca.

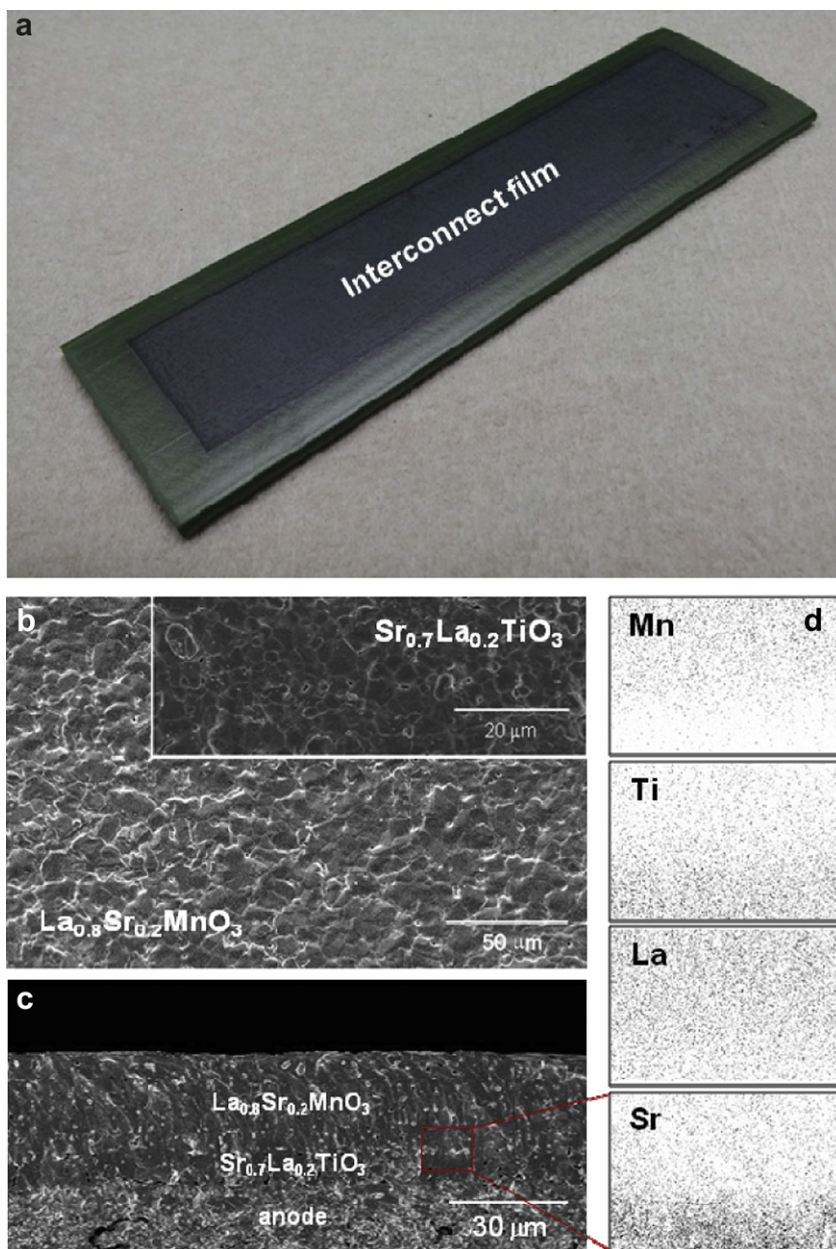


Fig. 2. (a) Anode-supported flat-tubular SOFC fabricated in this study. SEM images of (b) surface and (c) cross-section of the interconnect film co-sintered with the anode support at 1400 °C. (d) The atomic distributions in the interconnect film obtained by EDS analysis.

530 mΩ cm² at 750 °C (Fig. S5). Sr_{0.7}La_{0.2}TiO₃ is an n-type conductor and, at high oxygen partial pressures, the electrical conduction takes place by the movement of cation vacancies rather than by electron hopping. Therefore, Sr_{0.7}La_{0.2}TiO₃ exhibits very low electrical conductivity under oxidizing conditions on the cathode, resulting in an increased ASR in the dual atmosphere. The ASR measurements confirm that a combination of n-type Sr_{0.7}La_{0.2}TiO₃ and p-type La_{0.8}Sr_{0.2}MnO₃ layers leads to a reduced ASR of the interconnect film in a dual atmosphere. As shown in Fig. 3b, no significant increase of ASR was observed at 750 °C for 550 h of continuous testing. The SEM image (Fig. S6) taken from the tested specimen confirmed that the microstructure of the interconnect layer remained unchanged during the long-term stability test. It is known that La_{0.8}Sr_{0.2}MnO₃ decomposes into other phases, e.g. La₂O₃ and MnO, under highly reducing conditions, which

results in a drastic increase of resistance. According to the report by Mizusaki et al. [15], the critical oxygen partial pressures below which La_{0.8}Sr_{0.2}MnO₃ decomposes are approximately 10⁻¹⁵ Pa at 750 °C. The stability test indicates that for the optimized interconnect design, the dense Sr_{0.7}La_{0.2}TiO₃ layer effectively prevents direct exposure of La_{0.8}Sr_{0.2}MnO₃ to the reducing side and dissociation into less conducting phases.

Fig. 4a displays the polarization curves of the flat-tubular cell with the ceramic interconnect film measured at various temperatures. The open-circuit voltage (OCV) of ca. 1.0 V was observed, implying that the permeability of the interconnect film to gases is insignificant. Furthermore, the interconnect resistance was low, so that a power density as high as 360 mW cm⁻² was achieved with the anode-supported flat-tube cell made using the ceramic interconnect. In this work, a comprehensive optimization study has not

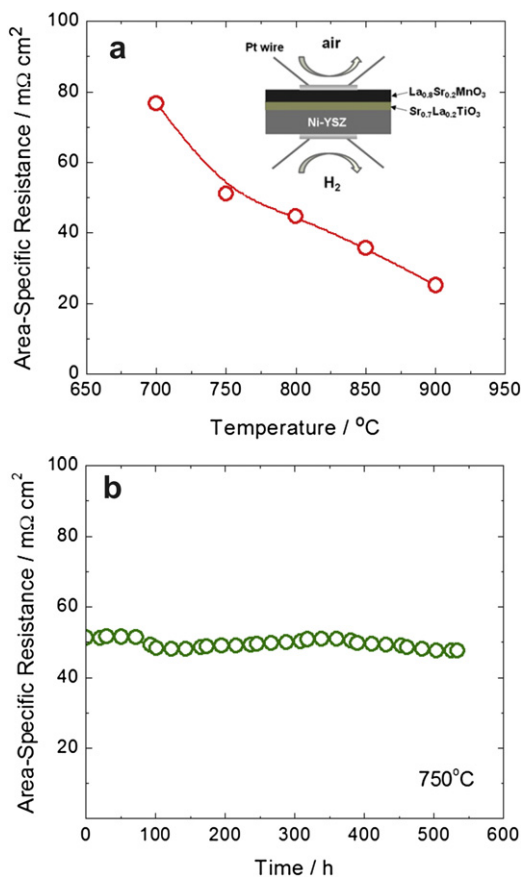


Fig. 3. (a) Area-specific resistances (ASR) of the interconnect film measured at various temperatures, and (b) ASR vs. time curve at 750 °C.

been carried out yet. Given the fact that the interconnect film shows low resistance (25 to 76 $\text{m}\Omega \text{cm}^2$), it is expected that further optimizations of the cell designs, the microstructures of electrode and electrolyte layers and the fabrication processes will lead to an improved cell performance. The optimization study is currently being carried out.

At this point, it is of interest to compare the performances of the flat-tubular SOFCs equipped with and without the interconnect film, in order to determine the performance loss due to the ceramic interconnect film. To measure the performance of the cell without the interconnect film, the current collection from the anode should be made either from an edge of the flat-tube or from metal (e.g. Pt or Ni) wires inserted into the holes of the anode support. Further complications, however, arise when different methods are used for the current collection, because ohmic polarization losses are strongly dependent on the current collecting method. In order to avoid any complications due to the current collection, the interconnect film was fabricated by using a highly conductive Ag-glass composite material (90:10 in weight). Ag-glass composites have been used as a conductive sealant for SOFCs [16,17], and the conductivity of the composite material with 10 wt.% glass was measured to be ca. 350 S cm^{-1} at 750 °C [17]. Since the Ag-glass composite becomes unstable due to the vaporization and agglomeration of Ag at high temperatures above 750 °C, only the cell performances at 750 °C were compared in Fig. 4b. The OCVs are almost the same for both cells, but the maximum power density of the SOFC with the $\text{Sr}_{0.7}\text{La}_{0.2}\text{TiO}_3/\text{La}_{0.8}\text{Sr}_{0.2}\text{MnO}_3$ interconnect film is slightly lower by 0.04 W cm^{-2} compared to that with the Ag-glass interconnect film.

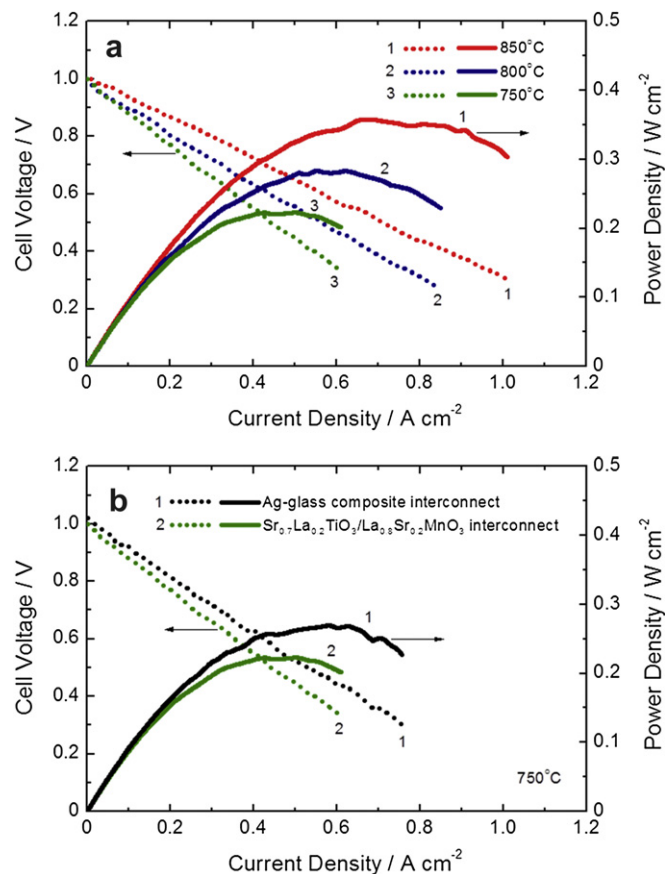


Fig. 4. (a) Polarization curves measured on the anode-supported flat-tubular SOFC with the ceramic interconnect film at various temperatures. (b) Polarization curves measured on the SOFCs with the Ag-glass composite and $\text{Sr}_{0.7}\text{La}_{0.2}\text{TiO}_3/\text{La}_{0.8}\text{Sr}_{0.2}\text{MnO}_3$ interconnect films at 750 °C.

4. Conclusion

An anode-supported flat-tubular SOFC with a highly conductive and dense interconnect film is developed. The dense interconnect film with $\text{Sr}_{0.7}\text{La}_{0.2}\text{TiO}_3$ on the anode side and $\text{La}_{0.8}\text{Sr}_{0.2}\text{MnO}_3$ on the cathode side is fabricated using the screen-printing process, followed by co-sintering with the anode and the electrolyte. The interconnect film is highly conductive and stable in a dual atmosphere.

Acknowledgments

This work was supported by the Materials Technology Development Program (Development of Highly Conductive Nano-composite Materials for Interconnects, Project No. 10037312) funded by the Ministry of Knowledge Economy (MKE, Korea).

Appendix A. Supplementary material

Supplementary material associated with this article can be found in the online version, at doi:10.1016/j.jpowsour.2012.04.025.

References

- [1] J.-H. Kim, R.-H. Song, K.-S. Song, S.-H. Hyun, D.-R. Shin, H. Yokokawa, J. Power Sources 122 (2003) 138–143.
- [2] T.-H. Lim, J.-L. Park, S.-B. Lee, S.-J. Park, R.-H. Song, D.-R. Shin, Int. J. Hydrogen Energy 35 (2010) 9687–9692.

- [3] T. Suzuki, B. Liang, T. Yamaguchi, K. Hamamoto, Y. Fujishiro, *Electrochem. Commun.* 13 (2011) 719–722.
- [4] B.-K. Park, J.-W. Lee, S.-B. Lee, T.-H. Lim, S.-J. Park, R.-H. Song, W.B. Im, D.-R. Shin, *Int. J. Hydrogen Energy* 37 (2012) 4319–4327.
- [5] W.Z. Zhu, S.C. Deevi, *Mater. Sci. Eng. A* 348 (2003) 227–243.
- [6] N. Sakai, H. Yokokawa, T. Horita, K. Yamaji, *Int. J. Appl. Ceram. Technol.* 1 (2004) 23–30.
- [7] H. Yokokawa, N. Sakai, T. Kawada, M. Dokiya, *J. Electrochem. Soc.* 138 (1991) 1018–1027.
- [8] M. Mori, Y. Hiei, N.M. Sammes, *Solid State Ionics* 135 (2000) 743–748.
- [9] J. Schoonman, J.P. Dekker, J.W. Broers, N.J. Kiewiet, *Solid State Ionics* 46 (1991) 299–308.
- [10] L.J.H. Kuo, S.D. Vora, S.C. Singhal, *J. Am. Ceram. Soc.* 80 (1997) 589–593.
- [11] R. Hui, Z. Wang, O. Kesler, L. Rose, J. Jankovic, S. Yick, R. Maric, D. Ghosh, *J. Power Sources* 170 (2007) 308–323.
- [12] W. Huang, S. Gopalan, *J. Power Sources* 154 (2006) 180–183.
- [13] H.-J. Son, R.-H. Song, T.-H. Lim, S.-B. Lee, S.-H. Kim, D.-R. Shin, *J. Power. Sources* 195 (2010) 1779–1785.
- [14] S.-S. Pyo, S.-B. Lee, T.-H. Lim, R.-H. Song, D.-R. Shin, S.-H. Hyun, Y.-S. Yoo, *Int. J. Hydrogen Energy* 36 (2011) 1868–1881.
- [15] J. Mizusaki, H. Tagawa, K. Naraya, T. Sasamoto, *Solid State Ionics* 49 (1991) 111–118.
- [16] X. Deng, J. Duquette, A. Petric, *Int. J. Appl. Ceram. Technol.* 4 (2007) 145–151.
- [17] S.-H. Pi, S.-B. Lee, R.-H. Song, J.-W. Lee, T.-H. Lim, S.-J. Park, D.-R. Shin, C.-O. Park, *Int. J. Hydrogen Energy*, submitted for publication.